Theor Chem Acc (2002) 107:187–199
DOI 10.1007/s00214-001-0309-7

Theoretical
Chemistry Accounts

Regular article

A lattice dynamics model for M_2XY_6 systems in the $Fm3m(O_h^5)$ space group

Roberto Acevedo, Ernesto Cortés

Facultad de Ciencias Físicas y Matemáticas, Universidad de Chile, Beauchef 850, Casilla, 2777 Santiago, Chile

Received: 12 May 2001 / Accepted: 11 September 2001 / Published online: 22 March 2002

Abstract. This work is about the development of a generalized dynamic model to account for both the short-range and the long-range interactions in M_2XY_6-type crystals in cubic environments. The short-range vibrational interactions are handled using a mixed force field, whereas the long-range interaction terms are worked out by employing a revised version of the Ewald method. In both cases, new criteria are introduced so as to get a more realistic overall picture of the lattice dynamics for these crystals. As for the short-range vibrational terms, a criterion is included to minimize the cross terms in the potential-energy distribution and in this way to include the idea of a natural potential-energy distribution. The Coulombic interaction terms are worked out and a new convergence test is introduced to make sure that the series expansion in both the direct and the reciprocal spaces converge at the same speed and simultaneously, preserving the electroneutrality of the system. The current model has been applied to Cs_2UBr_6; we have fitted the $\vec{k} = \vec{0}$ vibrational frequencies as well as the generation of the phonon dispersion curves for different polarization directions. As a result, the model is shown to have some utility and flexibility to handle this kind of complex calculation and could be generalized to more complex systems, such as elpasolite-type crystals, to test the validity of the approximations and constrains involved. We anticipate that many questions are still open to discussion and the need for more complete and accurate data is emphasized throughout the course of the current research work.

Key words: Lattice dynamics – Dispersion and phonon dispersion curves

1 Introduction

A general symmetry-adapted formalism is developed to model and rationalize both the short-range and the long-range interaction terms in an M_2XY_6-type system in cubic environments. A 15-particle model system is introduced to simulate crystals belonging to the $Fm3m(O_h^5)$ space group. Our current model has been worked out on the basis of a mixed Urey–Bradley force field and a general modified valence force field (UBFF–MGVFF) to describe the short-range interactions, together with a refined version of the Ewald method, used to account for the long-range interactions in the crystal. A major point in this work is a new convergence test to deal with the lattice sums, in both the direct and the reciprocal spaces, and a new criterion (based on a concept of natural potential-energy distribution, NPED) is also introduced to optimize the short-range interactions. Our current model avoids any supraparameterization since we feel that this latter scheme obscures both the physics and the chemistry of the problem we are aiming to solve. This generalized model is able to account for both short-range and long-range interaction terms between atoms belonging to the same and different unit cells. As a test of the current model, we have worked out an application to the Cs_2UBr_6 crystal, for which there is a reasonable database of very carefully obtained experimental data.

It is shown that the agreement between the theoretical predictions and the experiment is fairly good and the current model calculations are shown to have both some utility and some flexibility.

This formalism may be generalized to deal with more complicated systems, such as Cs_2NaLnZ_6, elpasolite-type systems (for which the beauty of the experimental data is such that it deserves finer theoretical work). As for the Cs_2UBr_6 crystal, the dispersion of the τ_{1u} symmetry-adapted normal modes of vibrations and that of the dispersion of the UBr_6^{2-} rotatory mode is reanalyzed on the basis of the current model. The model developed in the current research is compared with that of Torres et al. [1], who applied the theory of lattice dynamics in the harmonic approximation, using a rigid ion model due to Born and Huang [2]. This model calculation was applied to systems such as K_2SnBr_6, K_2PtBr_6, Cs_2SnBr_6 and Rb_2SnBr_6 crystals in the cubic phase.

Correspondence to: R. Acevedo
e-mail: lindsey@cec.uchile.cl

Phonon frequencies and the normal modes of vibrations at the zone center were obtained and some interesting conclusions were drawn from these calculations. Furthermore, many approximations were employed to deal with both the short-range and the long-range interaction terms, and these results provide a rather low value for the libration frequency of all the crystals studied. They also found that, within this approximation employed, their calculated parameters indicate that all these crystals are partially ionic. The model of these authors is different from ours in many respects, though we recognize that more theoretical and experimental work is necessary to draw some more solid conclusions. These authors suggested that the calculated vibrational frequencies and the normal modes of vibrations for the rotational τ_{1g} mode may be employed for future experimental and theoretical studies in determining elastic, dielectric or piezoelectric behavior as a function of structural phase transitions. We would rather focus our attention upon the development of both more general physical and generalized calculation models for spectral intensities so as to test the utility and flexibility of our current model calculations.

Here, we used as an application the Cs_2UBr_6 system, which is highly symmetric and is classified as transforming according to the symmetry operations of the $Fm3m(O_h^5)$-space group. The choice of this system to illustrate both the advantages and the disadvantages of the model to be introduced was influenced by several factors:

1. The crystal structure is well known and highly symmetric, corresponding to a cubic space group, where the U^{4+} ions occupy sites of essentially octahedral symmetry.
2. For this crystal, a fairly accurate database has been accumulated over the last 3 decades from both absorption and emission studies.
3. The f^2 energy level scheme gives rise to extensive, well-resolved absorption spectra spanning the region from the IR to the UV.
4. The strongest peaks in these spectra at different temperatures involve mainly $\Gamma_1 \rightarrow \Gamma_2 + \nu_k$ ($k = 3, 4, 6$) type excitations, with the explicit cooperation of odd parity normal modes of vibrations, with the exception of a few lines which can be explained on the basis of a magnetic dipole mechanism.

This system has thus provided extensive data to test calculation models of the *f*-electron crystal field [3, 4], of electronic [5] and vibronic spectral intensities [6], of vibronic interactions [7] and of lattice dynamics [1, 8, 9, 10, 11, 12, 13].

2 Model calculation and lattice dynamics

The dynamics equations for a general lattice may be written in matrix notation as [1, 9, 11, 13, 14, 15]

$$\mathbf{D}\left(\vec{k}\right)\mathbf{E}\left(\vec{k}\right) = \mathbf{E}\left(\vec{k}\right)\Omega^2\left(\vec{k}\right) \quad . \tag{1}$$

Here, $\Omega^2(\vec{k})$is a diagonal matrix, whose eigenvalues are denoted as w_{pk}^2, and $\mathbf{E}(\vec{k})$ stands for the matrix of the normalized eigenvectors $e_\alpha(\mu i|pk)$. Some relevant mathematical properties are as follows. The Fourier-transformed matrix $\mathbf{D}(\vec{k})$, whose elements are labeled as $D_{\alpha\beta}\left(\begin{matrix}\mu i \\ \nu j\end{matrix}\middle|\vec{k}\right)$, is known as the dynamic matrix and from its structure two properties of paramount importance are derived: $\mathbf{D}(\vec{k})^* = \mathbf{D}(-\vec{k})$ and $\mathbf{D}(\vec{k})^\dagger = \mathbf{D}(\vec{k})$.

As for the lattice dynamics of these types of luminescent materials, several studies with a variety of aims can be found in the literature [1, 9, 11, 13, 16, 17, 18]. In many of these studies, and owing to the complexity of both the physics and the mathematics involved in lattice-dynamics-type calculations, a parameterization criterion concerning the minimization of the mean error deviation among the observed and calculated vibrational eigenvalues was utilized. From the mathematical viewpoint an accurate fitting may be obtained, using appropriate optimization computing programs; nevertheless all these optimization procedures are most likely not to be able to guarantee that a global minimum may be reached during this optimization procedure.

It seems to us that some additional physical constraints should be included in these calculations and therefore any optimization procedure must incorporate these new criteria explicitly. The conclusions obtained, therefore, should be regarded as determined by these assumptions and constraints in the model calculation. We have never had and most likely will never have enough experimental data to perform an exact mathematical fitting; thus, it seems advisable to look for simple and flexible models to account for the obtained experimental data. A fairly good example is afforded by the normal coordinate analysis for a seven-atom system: Here the number of degrees of freedom is 15 and the number of unknown force constants is larger than the experimental data obtained from spectroscopic studies [19, 20, 21].

For this system, the normal modes of vibrations transform in the octahedral molecular point group as follows [11, 20]: $\Gamma_{\text{vib}} = \alpha_{1g}(\nu_1) + \varepsilon_g(\nu_2) + \tau_{1u}(\nu_3) + \tau_{1u}(\nu_4) + \tau_{2g}(\nu_5) + \tau_{2u}(\nu_6)$.

Thus, the $\tau_{1u}(2 \times 2)$ symmetry species is 2×2, and the associated potential-energy matrix involves three unknown symmetry-adapted matrix elements, F_{33}, $F_{34} = F_{43}$, F_{44}, which are themselves linear combinations of force constants involving internal coordinates (stretching and bending coordinates). For these systems, the most common information is the six vibrational frequencies ν_i ($i = 1, 2, 3, 4, 5, 6$) associated with the XY_6^{2-} ion, uncoupled to the motions of the counterion Cs^+ ($\tau_{1u} + \tau_{2g}$).

It is customary, in the literature, to solve the vibrational equations of motion $\mathbf{GFL} = \mathbf{L}\Lambda$, excluding long-range interactions contributions, and since $\mathbf{LL}' = \mathbf{G}$ it follows that $\mathbf{L}'\mathbf{FL} = \Lambda$. Here Λ is a diagonal matrix, whose elements are denoted as λ, where $\sqrt{\lambda_i} = \left(\frac{\bar{\nu}_i(\text{cm}^{-1})}{1303.16}\right)$. In our current notation, these matrix elements may be written in an expanded form as follows: $\lambda_i = \sum_{k=3,4} L_{ki}^2 F_{kk} + \sum_{k \neq l(3,4)} L'_{ik} F_{kl} L_{li}, i = 3, 4.$ It is

standard to perform the normal coordinate analysis, assuming that the off-diagonal terms, $\sum_{k\neq l(3,4)} L'_{ik}F_{kl}L_{li}$ are either negligible or zero (based upon the fact that it is expected that the off-diagonal **F**-matrix elements should be smaller when compared with the diagonal matrix elements). This kind of argument is unfortunately rather inaccurate since the **L**-matrix elements depend upon the details of the force field (F) and also let us add on the details of the optimization procedure chosen by different authors. The main point is that for most systems of spectroscopic interest, the experimental data available are rather scarce or limited, so we feel that it is not obvious that we should neglect these off-diagonal matrix elements, unless our optimization software includes a subroutine to minimize these cross terms (which may be regarded as some kind of interference terms).

Our strategy to perform the normal coordinate analysis for the $\tau_{1u}(2\times 2)$ symmetry block is as follows:

1. We define $k = \left(\frac{F_{44}}{F_{33}}\right)$ as a new fitting parameter to be fitted so as to minimize the magnitude of the cross terms for the potential-energy distribution. This k parameter relates essentially (weak coupling among the two τ_{1u} normal modes of vibrations) the frequencies of the bending to the stretching vibrations and the experimental evidence indicates that its value should range between 0 and 1.
2. The best possible k values are chosen so that they obey two criteria simultaneously: they produce sensible values for the internal force constants and they minimize the cross terms, producing a NPED. Thus, to a first approximation, we could regard this optimization criterion as a constraint upon the solutions or the vibrational equation of motions for the system.

As for the M_2XY_6-type systems, we have moved away from the seven-atom system and have defined a model (by no means unique!) made up of 15 atoms (Fig. 1). This more general physical overall picture of the crystal will allow us to include additional terms representing interactions among neighboring atoms which belong to different unit cells (interaction terms of the type M–X and M–Y) which, in principle, should provide a better and more comprehensive description of the terms involved in the dynamics matrix, as well as a better understanding of both the phonon dispersion curves and the electron–phonon interaction. Chodos and Berg [13] introduced for these types of crystals contributions due to nearest- and next-nearest-neighbor intercell Y–Y interactions in addition to M–M intercell interactions. In preliminary works on this subject, Chodos and Satten [9, 10] used seven parameters to fit a total of seven vibrational frequencies and many improvements were achieved in latter work by Chodos and Berg [13]. In spite of all these efforts, many fundamental questions are still open to discussion. We certainly recognize that a calculation of the shape of the vibronic absorption spectrum or a neutron scattering analysis of phonons should advance the state of the art for the understanding of these complex processes in solid-state physics. We have initiated a program along these two lines to fill the gap and to contribute new models and formalisms. A substantial amount of work is in progress in our laboratories with reference to elpasolite Cs_2NaLnZ_6-type systems. For further details, the reader is referred to work already published [1, 12, 21, 22, 23, 24, 25].

For systems such as M_2XY_6 in the $Fm3m(O_h^5)$ space group, the accepted nuclear equilibrium configuration may be found in Refs [8, 11, 25, 26] and references therein. The antifluorite structure is the same as that of CaF_2 and with reference to our chosen application to Cs_2UBr_6, the Ca^{2+} cations are replaced by UBr_6^{2-}, and F^- is substituted by Cs^+. Also $V_a = 2r_0^3$ is the volume of the unit cell and r_0 is half the absolute value of the reticular vector. For the $CsUBr_6$ system, we have $r_0 = 0.555$ nm[7]. Furthermore, a detailed discussion of the first Brillion zone (BZ) of face-centered-cubic systems is available in the literature and does not need to be repeated here [14, 15, 27, 28].

Generally speaking, the short-range and the long-range Coulombic contributions to the dynamical matrix may be summed up by writing the crystal field potential, V, as

$$V = \phi^{SR} + \varphi^{C} \quad . \tag{2}$$

For the sake of completeness, in the coming sections we give a brief discussion of these two contributions to the total crystal field potential.

2.1 Modeling of the short-range interactions

The short-range interactions in the whole crystal (Cs_2UBr_6), as will be shown, may be successfully modeled using a general version of the modified UBFF [11, 19, 26, 29, 30, 31]:

$$\begin{aligned} 2\phi^{SR} = {} & R_2^2 H \sum_{Br-U-Br} (\Delta\theta)^2 + K_q \sum_{Cs-Cs} (\Delta r)^2 \\ & + F \sum_{Br-Br} (\Delta r_1) + 2R_1 F' \sum_{Br-Br} (\Delta r_1) \\ & + K \sum_{U-Br} (\Delta r_2)^2 + 2R_2 f' \sum_{U-Br} (\Delta r_2) \\ & + K_m \sum_{Cs-Br} (\Delta r_3)^2 + 2R_3 f'' \sum_{Cs-Br} (\Delta r_3) \quad . \end{aligned} \tag{3}$$

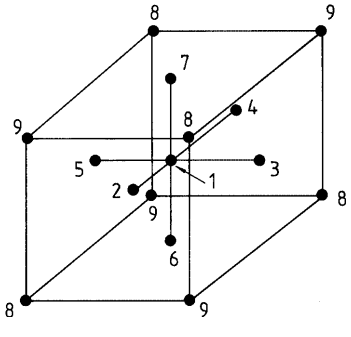

Fig. 1. Nuclei equilibrium positions for the Cs_2UBr_6 lattice

In this notation R_1, R_2 and R_3 stand for the nuclear equilibrium bond distances for the nuclei ion pairs Br–Br, U–Br and Cs–Br, respectively. K and H represent the main U–Br stretching and Br–U–Br bending force constants. K_q, K_m and f'' stand for interactions among particles belonging to different unit cells, and the F has been included to take into account linear interactions among bromine atoms. We must emphasize that the model used here is by no means unique and, of course, we recognize that there are other interactions which should be included in more sophisticated models for the lattice dynamics of these systems. At this stage of the discussion, we must take into account the experimental data available, and on the basis of this information choose a model calculation with a minimum set of parameters to be determined using a semiempirical calculation method. We also need to judge the quality of the fitting and therefore we need to elaborate sophisticated optimization computing programs so as to be able to discern among the various possible local minimum obtained in the point-to-point optimization procedures and eventually to be able to reach a global minimum. This is the strategy on top of the criterion, mean error deviation minimization so as to avoid compensation of errors. Thus, our approach in any calculation is to look for new constraints and convergence tests in order to critically test our model calculation against the experimental data.

2.2 Lattice sums and long-range interaction contributions

The actual evaluation of the Coulombic contribution to the total potential energy may be evaluated, taking into account the crystal sums over both the direct and the reciprocal spaces.

The previous statement should be handled with care. In order to retain the electric neutrality of the crystal, both summations must converge at the same speed and time. One valid approach to tackle this problem is to use a generalized Ewald calculation method. This formalism assumes that when both positive and negative Gaussian distributions are included in the model, the actual interaction with the lattice produces two potentials, say ϕ^G and $-\phi^G$, so the Coulombic potential can be written as

$$\phi^C = \phi^G + (\phi^C - \phi^G) = \phi^G + \phi^H \quad . \tag{4}$$

Once this partition is adopted, the Coulombic contribution to the dynamic matrix, that is

$$q_N q_M e^2 C_{\alpha\beta}\begin{pmatrix}\vec{k}\\ N\ M\end{pmatrix} = \sum_{l'} \phi^C_{\alpha\beta}\begin{pmatrix} l & l'\\ N & M\end{pmatrix} \exp\left[i\left(\vec{k}\cdot\vec{r}_{NM}\right)\right] \quad , \tag{5}$$

is expressed in terms of two series, one being defined in the direct space, N^H, associated with ϕ^H, and the other series defined in the reciprocal space, N^G, which is itself related to ϕ^G.

In Eq. (5), q_N stands for the electric charge of the nth particle in the lth unit cell, and α, $\beta = X$, Y, Z, i.e. the polarization directions along the Cartesian axis. Bearing this in mind and after some algebraic manipulations, Eq. (5) may be written in a more convenient form, namely [7, 11]

$$q_N q_M e^2 C_{\alpha\beta}\begin{pmatrix}\vec{k}\\ N\ M\end{pmatrix} = \left[N^G_{\alpha\beta}\begin{pmatrix}\vec{k}\\ N\ M\end{pmatrix} + N^H_{\alpha\beta}\begin{pmatrix}\vec{k}\\ N\ M\end{pmatrix}\right] - \delta_{NM}\sum_P\left[N^G_{\alpha\beta}\begin{pmatrix}0\\ N\ P\end{pmatrix} + N^H_{\alpha\beta}\begin{pmatrix}0\\ N\ P\end{pmatrix}\right] \quad , \tag{6}$$

where

$$N^G_{\alpha\beta}\begin{pmatrix}\vec{k}\\ N\ M\end{pmatrix} = \frac{4\pi q_N q_M e}{V_a}\sum_\tau \frac{\left(\vec{\tau}+\vec{k}\right)_\alpha \cdot \left(\vec{\tau}+\vec{k}\right)_\beta}{\left|\vec{\tau}+\vec{k}\right|^2} \times \exp\left\{-i\vec{\tau}.\left[\vec{r}\begin{pmatrix}0\\ M\end{pmatrix} - \vec{r}\begin{pmatrix}0\\ N\end{pmatrix} - \frac{\left|\vec{\tau}+\vec{k}\right|}{4\eta}\right]\right\} \tag{7}$$

and also

$$N^H_{\alpha\beta}\begin{pmatrix}\vec{k}\\ N\ M\end{pmatrix} = -\sum_{l',M}\left(\exp\left[i\left(\vec{k}\cdot\vec{r}\right)\right]\frac{\partial^2\phi^H\begin{pmatrix}\vec{r}\\ N\ M\end{pmatrix}}{\partial r_\alpha \partial r_\beta}\right)_0 . \tag{8}$$

In our current notation, $\phi^H\begin{pmatrix}\vec{r}\\ N\ M\end{pmatrix}$ is given by the identity:

$$\phi^H\begin{pmatrix}\vec{r}\\ N\ M\end{pmatrix} = 2q_N q_M e^2\left(\frac{\eta}{\pi}\right)^{1/2}\left(\frac{1}{r}\right)\int_r^\infty \exp\left(-\eta r'^2\right)\mathrm{d}r' \quad . \tag{9}$$

In this notation, η represents the width of the Gaussian, which was set at $\eta \cong r_0^{-2}$ in previous studies in this field [8, 10]. This is a point that should be elaborated with care, since the choice of this width is crucial with regards to the convergence of both series N^G and N^H. As we mentioned earlier in this section, these two series should both converge at the same speed and time, so as to preserve the charge neutrality of the crystal (this is indeed the basic idea of the forthcoming test for the convergence of these two series). It is important to observe that all the terms $\phi^C_{\alpha\beta}\begin{pmatrix} l & l'\\ N & M\end{pmatrix}$ in Eq. (5) are independent of the wave vector $\vec{k}$, so the long-range interactions are responsible for the dispersion between both the longitudinal and the transverse τ_{1u} modes for $\vec{k} \to 0$. With reference to the convergence test developed in this work, we observe that Eq. (4) holds only when the same number of Gaussians are employed to evaluate the long-range interactions in both $\Phi^G(N^G)$ and $\Phi^H(N^H)$ potentials. Owing to the fact that both series are defined over different spaces (the direct and the reciprocal spaces), they do not converge at the same speed and time, and it is necessary to make use of the relationship among

the vectors in both spaces and in this way obtain an appropriate value for the Gaussian width that will eventually produce the desired neutral overall charge in the whole crystal. Our calculation methods and strategy show that these two series converge approximately for a total of $6(3n+1)$ reciprocal vectors and $[(4n+1)^2 - 4n(2n+1)](4n+1) - 2n$ unit cells in the direct space. In this notation, the Gaussian width is expressed as $\eta \cong kr_0^{-2}$. In the particular case of the Cs_2UBr_6 crystal the convergence of the two series is reached for $k \cong 1.40$, which correspond to 32 vectors in the reciprocal space and 140 unit cells in the direct space.

3 Lattice sums: a convergence test

The convergence of the Coulombic contribution to the total potential energy depends critically upon the choice of the Gaussian width η [14]. In addition, the validity of Eq. (4) is fulfilled when the same number of Gaussians are employed to evaluate the long-range interactions in both the direct and the reciprocal spaces. It is well known that one of the main difficulties is that both series do not converge at the same speed, thus producing a charged density associated with the overall crystal. To avoid this crucial and outstanding inconvenience it seems sensible to employ a relationship among the vectors in both spaces to obtain an appropriate value for the Gaussian width that would produce a neutral charge in the crystal.

In passing, recall that a vector in the reciprocal space may be expressed in terms of the primitive translations in the reciprocal lattice, b_i ($i=1, 2, 3$) as follows: $\vec{r}_{h,k,l} = m(h\vec{b}_1 + k\vec{b}_2 + l\vec{b}_3)$, where the vectors $\vec{r}_{h,k,l}$ are perpendicular to the planes defined by the Miller indices (h, k, l) in the direct space. Furthermore, a constructive interference of rank m corresponds to interference between the origin plane and the parallel mth plane belonging to the family of planes labeled by the indices (h, k, l).

To a first approximation for a face-centered-cubic lattice, when the first two families of planes having the shortest distance among consecutive planes are taken into account, a convergence test for the two series is reached and any possible departure from the charge neutrality is prevented. In the limit and within this first approximation, the two series converge approximately for a total of $6(3n+1)$ reciprocal vectors and $(4n+1)[(4n+1)^2 - 4n(2n+1)] - 2n$ unit cells in the direct space. In this notation, the Gaussian width is given by $\eta \cong nr_0^{-2}$. For the sake of completeness, we report the families of planes, which were considered to develop the convergence test as just described.

1. Family 1 $\{(h, k, l) : (\pm 1, \pm 1, \pm 1)\}$.
2. Family 2 $\{(h, k, l) : (\pm 1, 0, 0), (0, \pm 1, 0), (0, 0, \pm 1)\}$.

We performed the lattice dynamics calculation with reference to Cs_2UBr_6 for the many reasons previously stated. For this lattice, the convergence test is reached for $n \approx 1.40$, corresponding to 32 vectors in the reciprocal space and a total of about 140 unit cells in the direct space.

4 Application to the Cs_2UBr_6 lattice in the $Fm3m(O_h^5)$ space group

The vibrational frequencies of a crystal depend upon the values of the wave vector, $\vec{k}$, along different polarization directions and this may be graphically represented in the phonon dispersion curves for the lattice. Three of these curves are classified as acoustic modes (the associated curves approach zero when $\vec{k} \to 0$). All the other curves are associated with optical modes, labeled as intermolecular (lattice vibrations) and intramolecular (moiety modes), and the zone center wave numbers of active modes may be determined from IR and Raman spectroscopy. The dispersion relationships will enable us to study, on an individual basis, the behavior of each phonon along various directions of the wave vector, classified according to the symmetry species of the reciprocal space. The criteria upon which we worked out the phonon dispersion curves are discussed in the coming sections.

4.1 The symmetry of the first BZ

The solutions of the equations of motion for a crystal are of the general form [11, 15, 27]

$$W_\alpha^{l,\mu,N} = A_\alpha^{\mu,N} \exp[i\left(\vec{k}.\vec{r} - wt\right) \tag{10}$$

and give rise to a set of periodic wave functions, in both space and time, which describe the vibrational state of a crystal associated with a traveling wave having a wavelength of $\left(\frac{2\pi}{|\vec{k}|}\right)$ and propagating along the $\vec{k}$ direction. These traveling waves are classified using symmetry arguments according to the wave vector. Furthermore, the periodic functions are linearly independent and since equivalent points in the reciprocal space correspond to the same solution, the set of periodic wave functions can be described completely within the first BZ.

The group associated with a wave vector $\vec{k}$ is defined as a set of operations in the factor group (subgroup of the corresponding space group), which leaves $\vec{k}$ invariant. To determine the number of points in the first BZ having the same energy, we must find the star associated with $\vec{k}$. This task may be achieved by performing all the operations of the factor group on the wave vector. Thus, in the first BZ, the number of functions, N_f, determined by symmetry to have the same energy is given by

$$N_f = (\text{order of the star of } \vec{k}) \times (\text{number of equivalent points to } \vec{k}) \ . \tag{11}$$

The symmetry information related to the first BZ in the space group O_h^5 is discussed in Refs [11, 16, 25] and will not be repeated for the sake of brevity.

4.2 Vibrational motions of the crystal: the Δ direction

The normal modes of vibration of a crystal may be classified using symmetry arguments according to the group of the wave vector $\vec{k}$. For a given direction within

the first BZ, the classification of the lattice normal modes may be obtained from the direct product: $S_v^{\vec{k}} = S_C \otimes S_E$, where $S_v^{\vec{k}}$ represents the space of the normal modes associated with the group of the wave vector $\vec{k}$, S_E corresponds to the space where the polarization vectors are rotated and S_C is the space in which the atoms are permuted within the unit cell by including an offset factor.

To span the S_E space, a Cartesian basis set is utilized, whereas to span the S_C space, we must work out the trace of a matrix representation corresponding to a $\hat{\gamma}$ operator acting on the vibrational displacement of an atom $\begin{pmatrix} l \\ M \end{pmatrix}$. As a result of this transformation, the atom is displaced to a new position described by the notation $\begin{pmatrix} l' \\ \gamma \quad M \end{pmatrix}$. Thus, the trace is given by the identity,

$$\chi_M(\hat{\gamma}) = \sum_M \delta_{M,\hat{\gamma}M} \times \exp\left[i\vec{k}_\gamma \cdot \vec{r}\begin{pmatrix} l & l' \\ M & \gamma M \end{pmatrix}\right] , \tag{12}$$

and

$$\hat{\gamma}\,\vec{k} = \vec{k} + \vec{k}_\gamma \tag{13}$$

In Eq. (12), the offset factor associated with the permutations is described by the exponential. In this formalism, the next step is to classify the set of equivalent atoms and to work out the traces corresponding to each of these sets. The normal modes of vibration of the crystal may then be classified in terms of the various irreducible representations of the wave vector. The symmetry coordinates of Cs_2UBr_6 at $\vec{k} = \vec{0}$ may be obtained from Ref. [11] and/or upon request from R.A.

For illustrative purposes, we have studied in detail the Δ direction in the reciprocal space of the crystal, with $\vec{k} = \pi(k_0, 0, 0)r_0^{-1}$ and $k_0\varepsilon(0, 1)$. In the C_{4v} molecular point group, the traces corresponding to the $\hat{\gamma}$ operator are such that in the subspace of the permutations, we find $S_C(U)\varepsilon A_1$, $S_C(Br^A)\varepsilon\, 2A_1$, $S_C(Br^B)\varepsilon A_1 + B_1 + E$, $S_C(Cs)\varepsilon A_1 + B_2$.

Also, in the rotation subgroup S_E, we find $S_E\varepsilon A_1(X) + E(Y,Z)$. Thus, the direct product space, $[S_v^{\vec{k}} = S_C \otimes S_E]$, gives rise to the following irreducible representations for the vibrational modes of the crystal along the Δ direction:

$$S_v^{\vec{k}}(U)\varepsilon A_1(X) + E(Y,Z) \ , \tag{14}$$

$$S_v^{\vec{k}}(Br^A)\varepsilon 2A_1(X) + 2E(Y,Z) \ , \tag{15}$$

$$S_v^{\vec{k}}(Br^B)\varepsilon A_1(X) + A_1(Y,Z) + B_1(X) + B_1(Y,Z) + A_1(Y,Z) + B_1(Y,Z) + E(X) + 2E(Y,Z) \ . \tag{16}$$

It is then straightforward, though long and tedious, to find the set of symmetry coordinates expressed in the basis set of the nuclear Cartesian displacement coordinates (see Appendix).

The advantage of this procedure is that the $E(\vec{k})$ matrix is unitary (see Eq. 1). The Δ direction is discussed further in Sect. 5.2.

4.3 A generalized force field description of the short-range interactions in the lattice

In Sect. 2.1, a modified UBFF (MUBFF) was introduced, and is used to simulate the short-range interactions among bonded and nonbonded atoms in the crystal, using as a basis a complete set of internal coordinates (stretching and bending coordinates).

From the geometry of the unit cell, the internal coordinate may be expressed as linear combinations of the corresponding nuclear Cartesian coordinates for each atom in the system [8, 9, 10, 11, 32, 33, 34].

This is achieved by employing the transformation matrix, $\boldsymbol{f}_x$:

$$\mathbf{M}^{-1/2}\boldsymbol{f}_X\mathbf{M}^{-1/2}\mathbf{R} = \mathbf{R}\Omega^2 \ . \tag{17}$$

In this transformation, the matrix elements of the diagonal **M** matrix correspond to the atomic masses of the system of particles in the crystal. The matrix $\boldsymbol{f}_x$ is finite in dimension, since equivalent atoms located in different unit cells may be included in the calculation with an offset factor depending upon the wave vector. Using the real, unitary matrix **P**, Eq. (17) may be rewritten as follows:

$$\mathbf{P}\mathbf{M}^{-1/2}\boldsymbol{f}_X\mathbf{M}^{-1/2}\mathbf{P}^{-1}\mathbf{P}\mathbf{R} = (\mathbf{P}\mathbf{R})\Omega^2 \ , \tag{18}$$

$$\left(\mathbf{P}\mathbf{M}^{-1/2}\right)\boldsymbol{f}_X\left(\mathbf{P}\mathbf{M}^{-1/2}\right)'(\mathbf{P}\mathbf{R}) = (\mathbf{P}\mathbf{R})\Omega^2 \ . \tag{19}$$

Next, it is convenient to introduce the $\boldsymbol{f}^P$ matrix, utilizing the transformation matrix

$$f^P = \left(\mathbf{P}\mathbf{M}^{-1/2}\right)\boldsymbol{f}_X\left(\mathbf{P}\mathbf{M}^{-1/2}\right)' \tag{20}$$

and it is straightforward to show

$$\boldsymbol{f}^P(\mathbf{P}\mathbf{R}) = (\mathbf{P}\mathbf{R})\Omega^2 \ . \tag{21}$$

Besides, for a given nuclear equilibrium configuration in the crystal, the internal coordinates are related to the nuclear Cartesian coordinates of each particle, and the symmetry coordinates of the system can be expressed in terms of the internal coordinates by means of the transformation $s = BR$ and also $S = Us = U(BR)$. This latter identity relates the space of the symmetry coordinates (S) to the space of the nuclear displacement Cartesian coordinates (R).

Thus, in terms of the transformation matrix (**UB**), we can rewrite Eq. (17) as follows:

$$\mathbf{G}_{sym}\mathbf{F}_{sym}\mathbf{L} = \mathbf{L}\Omega^2 \ , \tag{22}$$

where we have used the standard identities [11, 19, 20, 26, 30]

$$\mathbf{G}_{sym} = (\mathbf{U}\mathbf{B})\mathbf{M}^{-1}(\mathbf{U}\mathbf{B})' \ , \tag{23}$$

$$\mathbf{F}_{sym} = (\mathbf{U}\mathbf{B})'^{-1}\boldsymbol{f}_X(\mathbf{U}\mathbf{B})^{-1} \ , \tag{24}$$

$$\mathbf{L} = (\mathbf{U}\mathbf{B})\left(\mathbf{M}^{-1/2}\mathbf{R}\right) \ . \tag{25}$$

The set of equations (Eqs. 6, 23, 24, 25) represents the symmetrized form of the vibrational equations of motion for the system. Thus, the nontrivial solutions, for

an assumed force field (by no means unique), may be obtained by solving the secular determinant

$$\left|\mathbf{G}_{\mathrm{sym}}\mathbf{F}_{\mathrm{sym}} - \mathbf{\Omega E}\right| = 0 \ . \tag{26}$$

When this symmetry-adapted approach is used, it is a lot easier (for $\vec{k} = \vec{0}$) to deal with the internal modes of the UBr_6^{2-} complex ion and also to modify the MUBFF by including some extra-interactions of a GVFF type (UBFF–MGVFF). The basis set put forward in this research work includes both bonded and nonbonded interaction terms. It can be shown that these coordinates do not form a linearly independent set; nevertheless when a modified general force field is employed, the internal coordinate basis set does form both a complete and orthonormal set of coordinates.

4.4 Modeling and fitting of the observed vibrational wavenumbers

The relations among the GVFF and UBFF interactions for the UBr_6^{2-} complex ion, may be deduced from the comparison of Eq. (3) with the expression for the GVFF.

$$\begin{aligned} 2V = &\sum_{i=1-6} K_r(\Delta r_2)_i^2 + \sum_{j=1-12} H_\alpha(R_2\Delta\theta)_j^2 \\ &+ \sum_{j(l,k)=1-12} 2F_{rr}(\Delta r_2)_k(\Delta r_2)_l \\ &+ \sum_{p=1-6;j(p)=1-4} 2F_{r\alpha}(\Delta r_2)_p(R_2\Delta\theta)_{j(p)} \end{aligned} \tag{27}$$

It is straightforward to show that the following identities hold:

$$\begin{bmatrix} K_r = K + 2F + 2F' \\ H_\alpha = H + \frac{1}{2}(F - F') \\ F_{rr} = \frac{1}{2}(F - F') \\ F_{r\alpha} = \frac{1}{2}(F + F') \end{bmatrix} \ . \tag{28}$$

The stability condition is worked out from the fact that the first derivative of the potential energy with respect to the equilibrium nuclear Cartesian displacement coordinates should vanish identically, and the global minimum as for the potential energy is reached when the condition given in Eq. (29) is fulfilled:

$$f' + 4F' = 0 \tag{29}$$

This condition provides the exclusion of the linear terms of the potential-energy representation, which can then be written in matrix notation as follows:

$$2V = \mathbf{s}'\mathbf{f}\mathbf{s} \ . \tag{30}$$

Here **s** is the matrix of the internal coordinates and **f** is the potential-energy matrix, expressed in terms of interactions among these internal coordinates of the system. Furthermore, the set of internal coordinates may be expressed in terms of the Cartesian nuclear displacement coordinates, so we arrive to the identity: $2V = \mathbf{R}'\boldsymbol{f}_{\mathrm{x}}\mathbf{R}$, where $\boldsymbol{f}_{\mathrm{x}} = \mathbf{B}'\boldsymbol{f}\mathbf{B}$. Then, the $\boldsymbol{f}_{\mathrm{x}}$ matrix is expressed in terms of the Cartesian nuclear displacement coordinates of the system. We can go a step further and prove the identity $(\mathbf{UB})^{-1} = \mathbf{M}^{-1}(\mathbf{UB})'\mathbf{G}_{\mathrm{sym}}^{-1}$. By combining the previous set of equations; we can obtain the matrix elements associated with $\mathbf{F}_{\mathrm{sym}}$ as linear combinations of interactions of UBFF-type. The symmetrized **G** and **F** matrix elements are listed in Table 1.

The presence of the Cs atoms in our model leads to the inclusion of interactions among adjacent unit cells and when only the closest neighbors are considered,

Table 1. The symmetrized $\mathbf{G}_{\mathrm{sym}}$ and $\mathbf{F}_{\mathrm{sym}}$ matrices for the Cs_2UBr_6 lattices

G_{sym} matrix elements

$G_{1,1} = G_{2,2} = G_{3,3} = 0.01251$ $\quad$ $G_{4,4} = G_{6,6} = G_{8,8} = 0.02092$

$G_{4,5} = G_{6,7} = G_{8,9} = -0.01680$ $\quad$ $G_{4,19} = G_{6,20} = G_{8,21} = 0.00485$

$G_{5,5} = G_{7,7} = G_{9,9} = 0.05864$ $\quad$ $G_{5,19} = G_{7,20} = G_{9,21} = -0.00970$

$G_{10,10} = G_{11,11} = G_{12,12} = 0.05006$ $\quad$ $G_{13,13} = G_{14,14} = G_{15,15} = 0.02503$

$G_{16,16} = G_{17,17} = G_{18,18} = G_{25,25} = G_{26,26} = G_{27,27} = 1.00000$

$G_{19,19} = G_{20,20} = G_{21,21} = 0.00531$ $\quad$ $G_{22,22} = G_{23,23} = G_{24,24} = 0.00752$

F_{sym} matrix elements

α_{1g} symmetry

$F_{11} = K + 4f'' + 4F + f'_{\mathrm{r}} + 0.37118q_{\mathrm{Br}}^2 + 0.00714q_{\mathrm{Br}}q_{\mathrm{U}} - 0.03935q_{\mathrm{Br}}q_{\mathrm{Cs}}$

ε_g symmetry

$F_{11} = K + 4f'' + F + 3F' + F'_{\mathrm{r}} + 0.10362q_{\mathrm{Br}}^2 + 0.00714q_{\mathrm{Br}}q_{\mathrm{U}} + 0.003935q_{\mathrm{Br}}q_{\mathrm{Cs}}$

τ_{1g} symmetry

$F_{11} = 0.0125(2f'' + 2K_{\mathrm{m}} + f') - 0.00102q_{\mathrm{Br}}^2 - 0.00010q_{\mathrm{Br}}q_{\mathrm{U}} + 0.00111q_{\mathrm{Br}}q_{\mathrm{Cs}}$

τ_{2u} symmetry

$F_{11} = H + f' + K_{\mathrm{m}} + 0.5(F + F' + f') - 2t_2 - 0.03323q_{\mathrm{Br}}^2 - 0.00402q_{Br}q_{\mathrm{U}} + 0.04438q_{\mathrm{Br}}q_{\mathrm{Cs}}$

τ_{1u}^{TO}symmetry

$F_{11} = K + 0.05283f' + 4f'' + 2(F + F') - f'_r + 0.12590q_{\mathrm{Br}}^2 + 0.00714q_{\mathrm{Br}}q_{\mathrm{U}} - 0.03935q_{\mathrm{Br}}q_{\mathrm{Cs}}$

$F_{22} = H + 0.22777f' + f'' + K_{\mathrm{m}} + 0.5F - 1.5F' + 2t_2 + 0.03147q_{\mathrm{Br}}^2 - 0.00402q_{\mathrm{Br}}q_{\mathrm{U}} + 0.04438q_{\mathrm{Br}}q_{\mathrm{Cs}}$

$F_{33} = 0.4384f' + 12(2f'' + K_{\mathrm{m}}) + 0.41451q_{\mathrm{Br}}q_{\mathrm{Cs}} + 0.06705q_{\mathrm{U}}q_{\mathrm{Cs}}$

$F_{12} = 0.10970f' + 2F_{r\alpha} + F + F' + 0.06295q_{\mathrm{Br}}^2$

$F_{13} = 0.15220f' - 6.92284f'' + 0.06815q_{\mathrm{Br}}q_{\mathrm{Cs}}$

$F_{23} = 0.31601f' + 3.46409(f'' + K_{\mathrm{m}}) - 2.82843t_{\mathrm{b1}} + 0.15374q_{\mathrm{Br}}q_{\mathrm{Cs}}$

$F_{44} = 0.0407f'$

τ_{2g} symmetry

$F_{11} = H - 2t_1 + 0.25f' + 0.5(f'' + K_{\mathrm{m}} + F - F') + 0.02429q_{\mathrm{Br}}^2 - 0.00201q_{\mathrm{Br}}q + 0.02235q_{\mathrm{Br}}q_{\mathrm{Cs}}$

$F_{22} = 4K_{\mathrm{q}} + 8f'' + 4K_{\mathrm{m}} + 0.13817q_{\mathrm{Br}}q_{\mathrm{Cs}} + 0.05012q_{\mathrm{Cs}}^2 + 0.02235q_{\mathrm{U}}q_{\mathrm{Cs}}$

$F_{12} = -\sqrt{2}(f'' - K_{\mathrm{m}}) + 2.30939t_{\mathrm{bl}} + 0.10179q_{\mathrm{Br}}q_{\mathrm{Cs}}$

the number of Cs atoms to be included in the calculation amounts to 342 in total. However, when the temporal offset of the interactions involving the Cs atoms is worked out (including Cs–Cs, Cs–U and Cs–Br interactions), it is then possible to write the $\boldsymbol{f}_x$ matrix in terms of the interactions among the nine different kind of atoms, namely U: 1, Br: 2–7 and Cs: 8, 9. The additional GVFF type interactions and force constants included in the MUBFF employed in this study are

1. The stretch–bend interaction in UBr_6^{2-}, $F_{r\alpha}$.
2. The linear stretch–stretch interaction in UBr_6^{2-}, f_r' .
3. The bend–bend interaction of the type UBr_6^{2-}–Cs^+, t_{b1}.
4. The cis bend–bend interactions of UBr_6^{2-}, t_2.
5. The coplanar bend–bend interactions of UBr_6^{2-}, t_1.

The potential-energy stability becomes

$$R_{U-Br}(f' + 4F') + R_{Cs-Br}(4bf'') + \left(\frac{\partial \phi^C}{\partial \alpha_i}\right) = 0 \ , \qquad (31)$$

where $\alpha = X$ $(i = 2, 4)$, Y $(i = 3, 5)$, Z $(i = 6, 7)$. This approximation implies that the total resulting force on the bromide particles vanishes identically. In the present study, we set $b = 0$.

The secular determinant can be partitioned in subdeterminants of smaller dimensions. For the 1×1 symmetry blocks, the evaluation of the $\mathbf{F}_{sym}$ matrix elements is straightforward at the nuclear equilibrium configuration. For both the $\tau_{1u}(4 \times 4)$ and the $\tau_{2g}(2 \times 2)$ symmetry blocks the complexity of the problem increases substantially and in order to obtain the most appropriate and representative description of the force field for the physical model assumed for the crystal we need to include some additional physical constrains upon the various possible approximate solutions. We have discussed (Sect. 2) the concept of NPED in detail, and so need not repeat the discussion here. It is also necessary to add that a further criterion utilized to optimize the fitting consisted of the minimization of those short-range interaction force constants which are expected (from both knowledge and experience in normal coordinate analysis for polyatomic systems) to be either small or negligible. This criterion was utilized to estimate the value of the f'' force constant, which describes linear interaction terms [11].[1] These terms are small, but not zero, and their evaluation is very sensitive to the approximations involved in the model. Our experience indicates that a fairly good approach to this problem is to look for a global minimum for the overall potential energy with respect to a reaction coordinate.

[1] Fortran programs using a 15-atom-system model and a generalized force field (mixed UBFF–GVFF) to describe the short-range interactions for the M_2XY_6 systems can be obtained upon request from R.A

5 Results of the calculations and discussion

5.1 The Γ point $[\vec{k} = (0, 0, 0)]$

A factor group analysis [11, 26, 29, 35], for the Cs_2UBr_6 lattice gives the following projections into the octahedral molecular point group:

$$\begin{aligned}
&\Gamma\left(\text{translation: } UBr_6^{2-}\right) \varepsilon \tau_{1u}, \\
&\Gamma\left(\text{rotation: } UBr_6^{2-}\right) \varepsilon \tau_{1g}, \\
&\Gamma\left(\text{vibrational: } UBr_6^{2-}\right) \varepsilon \alpha_{1g} + \varepsilon_g + 2\tau_{1u} + \tau_{2g} + \tau_{2u}, \qquad (32) \\
&\Gamma(\text{Cs}) \varepsilon \tau_{2g} + \tau_{1u}, \\
&\Gamma(\text{acoustic}) \varepsilon \tau_{1u} \ ,
\end{aligned}$$

Thus, the Raman and IR active modes (i.e. for a zero temporal offset among unit cells) give rise to $\Gamma_{vib}(\vec{k} = 0) = \alpha_{1g}(\text{Raman}) + \varepsilon_g(\text{Raman}) + \tau_{1g} + 3\tau_{1u}(\text{IR}) + 2\tau_{2g}(\text{Raman}) + \tau_{2u}(-)$. The inclusion of both the short-range and the long-range interactions for Cs_2UBr_6 produces a fit as good as could be expected from this model calculation. It is worth mentioning that our strategy is to develop sensible physical models with a number of independent constraints so as to advance the state of the art in solid-state physics. Our calculation was not meant to fit the observed and the calculated vibrational wave numbers exactly; we would prefer to keep a simple model with a few parameters to be fitted from available experimental data. In Table 2, we list for this system the observed and calculated vibrational frequencies for $\vec{k} = \vec{0}$ and as the reader will notice the database has been updated, with new data provided kindly to us by P.A. Tanner. The magnitudes of the set of 13 force constants and the atomic charges on each particle are compared with previous results available

Table 2. $\vec{k}' = 0$, observed and calculated vibrational wave numbers of Cs_2UBr_6

Wave number (cm^{-1})		Symmetry coordinate assignment	F_{ij}^{sim}
ν_{obs}[a]	ν_{cal}		
197	197	α_{1g}:S_1	F_{11} = 182.61
(166)[b]	152	ε_g:S_4	F_{11} = 108.72
(56)[b]	53	τ_{2u}:S_{13}	F_{11} = 6.609
no	19	τ_{1g}:S_{16}	–
195	195	τ_{1u}^{TO}:S_6	F_{11} = 102.01
84	84	S_7	F_{22} = 10.57
51	51	S_{20}	F_{33} = 44.58
0[c]	0[c]	S_{25}	F_{12} = 0
			F_{13} = −6.8
			F_{23} = 6.0
			F_{44} = 0.0
87	87	τ_{2g}:S_{10}	F_{11} = 8.90
43	43	S_{22}	F_{22} = 14.47
			F_{12} = 0.0
(212)[b]	203	τ_{1u}^{TO}:S_6	
(87)[b]	94	S_7	
no	67	S_{20}	
no	0[c]	S_{25}	

[a] Ref. [10]
[b] Data provided by P.A. Tanner
[c] Acoustic mode

(using different approximations and another physical model) in the literature for this system [10] in Table 3. The values are generally similar, but with some remarkable exceptions. Our model predicts a reduction of the U–Br stretching force constant, the magnitude of K being only 63% of that obtained using a seven-parameter model [10]. Simple UBFF and MUBFF calculations for UBr_6^{2-} give a value for K of about 90 Nm^{-2}, and the magnitude is expected to decrease with the inclusion of further interactions in the model. Labonville et al. [19] pointed out that a decrease in K corresponds to a less stable anion structure, correlating with an increase in the repulsion constant, F. The force constant F' is smaller in magnitude than the value determined by Chodos and Satten [10] and of opposite sign to the convention where it is equated to $-0.10F$ [19]. The UBr_6^{2-} bending interaction parameters, which were introduced in this model, turn out to be of minor importance. Also, the trans strech–strech parameter is approximately midway between the values calculated for the UBr_6^{2-} moiety alone, using the GVFF and the MUBFF. The UBr_6^{2-} stretch–bend interaction constant, $F_{r\alpha}$, has a more significant value than that calculated from the single ion force field alone.

It is interesting that the model predicts a much lower wave number for the τ_{1g} rotational mode than the seven-parameter model [10]. The latter model calculates the rotational mode of the Cs_2MnF_6 lattice to be at 150 cm^{-1}; this unexpected value can be rationalized on the basis that the inclusion of additional short-range interactions among adjacent unit cells would reduce it. For K_2ReCl_6 [12], the calculated magnitude of the rotational mode was also much higher than the experimental value of about 26 cm^{-1}. The mode is sensitive to the halogen mass, so the wave number for Cs_2UBr_6 is indeed expected to be lower.

The $\vec{k} = \vec{0}$ wave numbers of UBr_6^{2-} may also be deduced from the vibronic spectra of the anion, when diluted into transparent host lattices. Many transitions have been studied in the electronic absorption [4] and emission [36] spectra and the wave numbers of the τ_{1u} modes S_6 and S_7 (from vibronic origins), the $\alpha_{1g}(S_1)$ and $\tau_{2g}(S_{10})$ modes (from progressions) are similar to those in Table 2. The effects of dispersion and coupling of modes to the host lattices are evidently apparent at $x = 0.05$ in $Cs_2Zr_{1-x}U_xBr_6$ since the $\tau_{2u}(S_{13})$ mode exhibits multiple structure, with the strongest feature near 60–64 cm^{-1}. Besides, two very weak bands near 160 and 166 cm^{-1} are observed in the vibronic sidebands and these are attributed to the zone boundary modes derived from $S_4(\varepsilon_g)$ (see Sect. 5.3). This suggests that the observed wave numbers for S_4, which was extrapolated (Eq. 8) from the Raman spectrum of Cs_2UCl_6, is about 10 cm^{-1} too low. The transverse optic–longitudinal optic (LO) splitting of the τ_{1u} modes is not, however, apparent in the spectra of the dilute crystals.

When the effective charges on the particles are allowed to vary in the fitting procedure, their variations do not produce major changes in the optimized wave numbers; however, small changes in the short-range interaction force constants may produce a rather inconsistent set of atomic charges on the particles in the crystal. This theoretical evidence should lead us to exploit new models and also to employ more sophisticated software to perform the optimization procedure. This optimization procedure should be carried out point to point for a given nuclear configuration and we would also need to make substantial improvement to the vibronic line shapes and the hyper-potential-energy surfaces of the terminal electronic states.

More theoretical work is needed and new models should be made available. A family of systems we are working on is the elpasolite type, for which a substantial number of highly accurate and careful measurements is available from different research groups.

Table 3. Calculated force constants and atomic charge for Cs_2UBr_6. The magnitude of q_{Cs} was constrained at 1.0. Also $2q_{Cs} + q_U + 6q_{Br} = 0$

Force constant	Magnitude (Nm^{-1})	
	This study	Ref. [9]
K	64.23	102
F	22.15	18
H	−4.55	−5
F'	0.35	−1
K_m	4.04	5.2
K_q	−1.35	−1.57
K'_q	0.0	–
f''	0.43	–
$F_{r\alpha}$	−12.25	–
f'_r	14.60	–
t_{b1}	0.28	–
t_2	0.65	–
t_1	−0.32	–
Particle	Magnitude (e^{-1})	
qBr	−0.5644	−0.525
qU	(1.3864)	(1.15)
qCs	(1.0)	(1.0)

5.2 The Δ direction: $[\vec{k} = \pi(k_0, 0, 0)r_0^{-1}]$ with k_0, $\varepsilon(0, 1)$

For this direction of the reciprocal lattice, the dynamical matrix may be partitioned using C_{4v} symmetry. The normal modes transform according to the following irreducible representations: $\Gamma(\text{vib} : \Delta)\varepsilon 6\alpha_1 + 2\beta_1 + \alpha_2 + 2\beta_2 + 8\varepsilon$.

The symmetrized short-range interaction force constants are tabulated in the Appendix and the long-range interactions for each symmetry species were evaluated for $0 < k_0 < 1$. The calculated frequencies for the various symmetry species along the Δ direction and for k_0, $\varepsilon(0, 1)$ are displayed in Table 4.

The most interesting results in this table are the relative large dispersions along the Δ direction of some of the phonons derived from the $\tau_{1u}(\Gamma)$ LO modes. The dispersion is relatively small for the UBr_6^{2-} τ_{1u} stretch, but is about 10 cm^{-1} for the τ_{1u} bend. The τ_{1u} vibronic sidebands of the electronic spectra of Cs_2UBr_6 exhibit broad triangular-shaped features between 85 and 90 cm^{-1} and between 197 and 217 cm^{-1}, peaking at 87 cm^{-1} and 211 cm^{-1}, respectively, which may therefore be assigned to the τ_{1u} LO modes.

5.3 Phonon dispersion curves for the Cs_2UBr_6 lattice

To obtain the phonon dispersion curves, we followed the same procedure as for the Δ direction (Sect. 5.2). In the space spanned by the wave vector $\vec{k}$. The descent of symmetry was handled using the compatibility tables given in the Appendix. The resultant phonon dispersion curves are given in Fig. 2.

The inclusion of extra interaction terms in the dynamical matrix $\mathbf{D}(\vec{k})$ produces a modification of the dispersion of the τ_{1u} modes with respect to the previous calculation [10]. This modification has been assumed to be derived from interactions among neighboring atoms corresponding to different unit cells in the lattice (U–Cs- and Br–Cs-type interactions). At some zone borders parity changes are observed. This is the case for the $\tau_{2g}(\Gamma)$ mode at X_5^- and X_2^- (X).

Additionally, modes of the same symmetry repel each other, this behavior being particular evident for the Λ and the Σ directions. For the τ_{2g} and the τ_{2u} modes, it is seen that a quasi-accidental degeneracy at the borders of the zones W (W_1 and W_2'') is observed, and this may be a consequence of the use of a mixed GVFF–UBFF to describe the vibrational behavior of the lattice.

6 Conclusions

The model employed in this work to fit the $\vec{k} = \vec{0}$ vibrational modes of the Cs_2UBr_6 crystal and the strategy used to produce the phonon dispersion curves for different polarization directions may be compared with the work reported by Chodos and coworkers [8, 9, 10, 13] and by other workers [35, 36, 37, 38, 39]; the major difference being that the force field has been symmetrized. Besides, our model is extended to include a total of 15 atoms, and therefore additional interaction terms and contributions have been incorporated, using a mixed UBFF–GVFF. Furthermore, several additional optimization criteria have been utilized in the fitting procedure. The terms not included in our current model represent interactions between Br particles belonging to different UBr_6^{2-} species. The inclusion of these interactions would require a major modification in our model calculation, by incorporating the 12 closer neighboring cells into our reference unit cell.

The model has been extremely successful to reproduce (with a minimum set of fitting parameters) the experimental $\vec{k} = \vec{0}$ vibrational wave numbers, and provides a better estimate of the τ_{1g} rotational wave

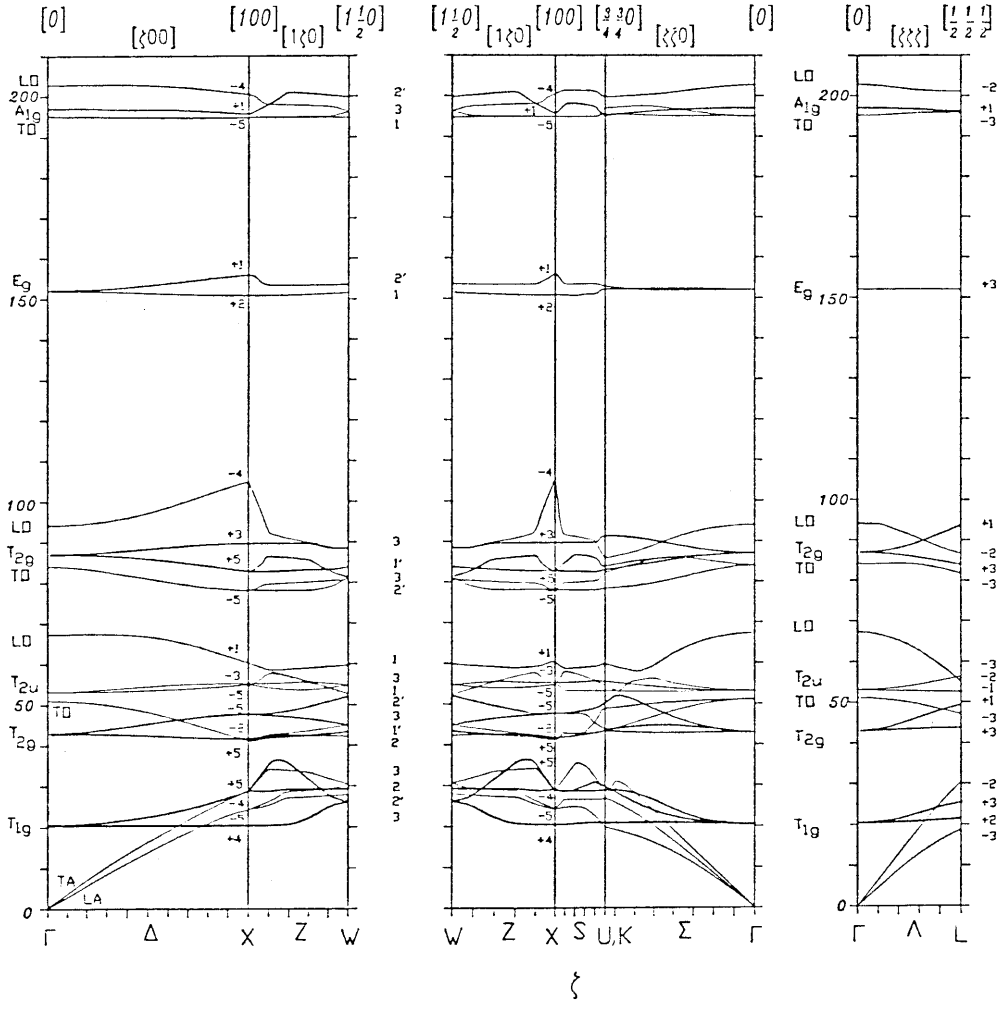

Fig. 2. Phonon dispersion curves for Cs_2UBr_6

Table 4. Calculated vibrational frequencies in the Δ direction

Symmetry	Wave numbers corresponding to κ_0					
	0.1	0.2	0.4	0.6	0.8	0.95
Δ_1	197.0	197.0	196.9	196.7	196.3	195.8
	152.1	152.2	152.9	153.8	154.9	155.7
	202.7	202.8	202.8	202.4	202.6	202.7
	94.1	94.4	95.8	98.4	101.7	104.1
	67.2	67.2	67.0	65.8	63.4	61.0
	3.5	6.9	13.2	18.9	24.0	27.6
Δ_2	152.0	151.9	151.5	151.2	151.0	150.8
	53.1	53.3	54.0	54.7	55.1	55.1
Δ_1	20.4	20.4	20.4	20.4	20.4	20.4
Δ_2'	87.1	87.2	87.9	88.7	89.4	89.7
	43.0	42.9	42.7	42.2	41.8	41.7
Δ_5	20.5	20.8	21.7	23.3	25.6	27.9
	53.0	53.0	53.1	53.4	53.9	54.4
	87.0	86.8	86.3	85.3	84.1	83.1
	43.1	43.4	44.6	46.0	47.1	47.6
	195.0	195.0	194.9	194.8	194.8	194.8
	83.8	83.4	81.8	80.1	78.8	78.1
	50.9	50.6	49.2	46.9	44.1	41.8
	2.8	5.6	11.1	16.2	20.8	23.6

number. In view of the improvement, this method can be generalized to perform lattice dynamic calculations for more complex systems, such as elpasolite-type crystals. A substantial amount of work in this direction is in progress in our laboratory. The choice of these systems has been influenced owing to the wealth of new and updated experimental data from both linear and nonlinear optics. Throughout the course of the present work, we introduced several additional constraints upon both the short-range and the long-range interactions, so as to make the model more realistic, though we recognize that there are still many questions open for discussion as well as some obscure points which need some clarification based upon solid calculations employing an accurate and reliable database. Finally, we strongly believe that elpasolite-type systems should be more conclusive to determine the utility and validity of these model calculations than other systems in this complex but fascinating field of research.

Acknowledgements. The authors express their gratitude to Fondecty for grant 1981207 to R.A.E.C. acknowledges both the Universidad de Chile and Fondecty, bodies which supported his studies to complete MSc and DSc degrees at the Facultad de Ciencias Físicas y Matemáticas of the Universidad de Chile. R. Tabensky is gratefully acknowledged for many highly illuminating suggestions for improvement of this work.

Appendix

The symmetry coordinates in the C_{4v} molecular point group are as follows:

Δ_1 symmetry
$S_1 = x_1$,
$S_2 = a(x_2 + x_4)$.
$S_3 = a(x_2 - x_4)$.
$S_4 = a^2(x_3 + x_5 + x_6 + x_7)$.
$S_5 = a^2(y_3 - y_5 - z_6 + z_7)$.
$S_6 = a(x_8 + x_9)$.

Δ_1 symmetry
$S_7 = a^2(x_3 + x_5 - x_6 - x_7)$,
$S_8 = -a^2(y_3 - y_5 + z_6 - z_7)$.

$\Delta_{1'}$ symmetry
$S_9 = a^2(z_3 - z_5 - y_6 + y_7)$.

$\Delta_{2'}$ symmetry
$S_{10} = -a^2(z_3 - z_5 - y_6 + y_7)$,
$S_{11} = a(x_8 - x_9)$.

Δ_5 symmetry
θ components
$S_{12} = a(y_2 + y_4)$,
$S_{13} = a(y_3 + y_5)$,
$S_{14} = a(y_6 + y_7)$,
$S_{15} = a(y_8 - y_9)$,
$S_{16} = y_1$,
$S_{17} = a(z_2 - z_4)$,
$S_{18} = a(x_6 - x_7)$,
$S_{19} = a(y_8 + y_9)$.

ε components
$S_{20} = a(z_2 + z_4)$,
$S_{21} = a(z_6 + z_7)$,
$S_{22} = a(z_3 + z_5)$,
$S_{23} = a(z_8 - z_9)$,
$S_{24} = z_1$,
$S_{25} = a(y_2 - y_4)$,
$S_{26} = -a(x_3 - x_5)$,
$S_{27} = a(z_8 + z_9)$,

Where $a = \sqrt{\frac{1}{2}}$

The symmetrized **F**-matrix elements of the Δ direction are

$$F_{11} = \left(\frac{8H + 2K - 2f_r' - 16F_{r\alpha} + 16t_2 + \frac{32t_{b1}}{\sqrt{6}} - 16F'}{m_U}\right) ,$$

$$F_{12} = -\left(\frac{\sqrt{2}\left(K - f_r' - 4F_{r\alpha}\right)}{\sqrt{m_U m_{Br}}}\right) ,$$

$$F_{14} = -\left(\frac{4H - 4F_{r\alpha} + 8t_2 + \frac{8t_{b1}}{\sqrt{6}} - 6F'}{\sqrt{m_U m_{Br}}}\right) ,$$

$$F_{16} = -\left(\frac{\frac{8t_{b1}}{\sqrt{3}}\cos\left(k_0\frac{\pi}{2}\right)}{\sqrt{m_U m_{Br}}}\right) ,$$

$$F_{22} = \left(\frac{4\left(2A^2 f'' + D^2 K_m\right) + K + 2(F + F') - f_r'}{m_{Br}}\right) ,$$

$$F_{24} = -\left(\frac{\sqrt{2}(F + F' + 2F_{r\alpha})}{m_{Br}}\right) ,$$

$$F_{26} = -\left(\frac{4\left(2A^2 f'' + D^2 K_m\right)}{\sqrt{m_{Br} m_{Cs}}}\right) ,$$

$$F_{33} = \left(\frac{4\left(2A^2 f'' + D^2 K_m\right) + K + 2(F + F') + f_r'}{m_{Br}}\right) ,$$

$$F_{35} = \left(\frac{\sqrt{2}(F - F')}{m_{Br}}\right) ,$$

$$F_{44} = \left(\frac{4f''\left(1 - A^2\right) + 4A^2 K_m + 2H + f' + F - 3F' + 4t_2}{m_{Br}}\right) ,$$

$$F_{46} = \left(\frac{4\sqrt{2}\left[A^2 K_m + f''\left(1 - A^2\right) - \frac{t_{b1}}{\sqrt{6}}\right]\cos\left(k_0\frac{\pi}{2}\right)}{\sqrt{m_{Br} m_{Cs}}}\right) ,$$

$$F_{55} = \left(\frac{4\left(2A^2 f'' + D^2 K_m\right) + K + 3F + F' + f_r'}{m_{Br}}\right) ,$$

$$F_{66} = \left(\frac{8f'' + 4K_m + 2K_q[1 - \cos(k_0\pi)]}{m_{Cs}}\right) .$$

– Δ_2 symmetry:

$$F_{77} = \left(\frac{4f''\left(1 - A^2\right) + 4A^2 K_m + 2H + F + F' - f' - 4t_2}{m_{Br}}\right) ,$$

$$F_{88} = \left\{\frac{8A^2 f'' + 4D^2 K_m + K + F + 3F' + f_r'}{m_{Br}}\right\} .$$

– Δ_1' symmetry:

$$F_{99} = \left(\frac{4f''\left(1 - A^2\right) + 4A^2 K_m + f'}{m_{Br}}\right) .$$

– Δ_2' symmetry:

$$F_{10,10} = \left(\frac{4f''\left(1 - A^2\right) + 4A^2 K_m + 4H + 2(F - F') - f' - 8t_1}{m_{Br}}\right) ,$$

$$F_{10,11} = \left(\frac{4\sqrt{2}\left[A^2(f'' - K_m) - 2t_{b1}\right]\cos\left(k_0\frac{\pi}{2}\right)}{\sqrt{m_{Br} m_{Cs}}}\right) ,$$

$$F_{11,11} = \left(\frac{8f'' + 4K_m + 2K_q[1 + \cos(k_0\pi)]}{m_{Cs}}\right) .$$

– Δ_5^θ symmetry:

$$F_{12,12} = \left(\frac{4f''\left(1 - A^2\right) + 4A^2 K_m + 2H + F + F' + f'}{m_{Br}}\right) ,$$

$$F_{12,13} = \left(\frac{F + F' + 2F_{r\alpha}}{m_{Br}}\right) ,$$

$$F_{12,14} = \left(\frac{4t_2 - 2F'}{m_{Br}}\right) ,$$

$$F_{12,16} = -\left(\frac{2\sqrt{2}\left(2t_2 - 2F' + H - F_{r\alpha} + \frac{2t_{b1}}{\sqrt{6}}\right)}{\sqrt{m_U m_{Br}}}\right) ,$$

$$F_{12,19} = \left(\frac{4f''\left(1 - A^2\right) + 4A^2 K_m + \frac{4t_{b1}}{\sqrt{6}}}{\sqrt{m_{Br} m_{Cs}}}\right) ,$$

$$F_{13,13} = \left(\frac{8A^2 f'' + 4D^2 K_m + K + 2(F + F') - f_r'}{m_{Br}}\right) ,$$

$$F_{13,14} = \left(\frac{F + F' + 2F_{r\alpha}}{m_{Br}}\right) ,$$

$$F_{13,16} = -\left(\frac{\sqrt{2}\left(K + f_r' - 4F_{r\alpha}\right)}{\sqrt{m_U m_{Br}}}\right) ,$$

$$F_{13,19} = \left(\frac{\left(8A^2 f'' + 4D^2 K_m\right)\cos\left(k_0\frac{\pi}{2}\right)}{\sqrt{m_{Br} m_{Cs}}}\right) ,$$

$$F_{14,14} = \left(\frac{4f'\left(1 - A^2\right) + 4A^2 K_m + 2H + F - F' + f'}{m_{Br}}\right) ,$$

$$F_{14,16} = -\left(\frac{2\sqrt{2}\left(2t_2 - 2F' + H - F_{r\alpha} + \frac{2t_{b1}}{\sqrt{6}}\right)}{\sqrt{m_U m_{Br}}}\right) ,$$

$$F_{14,19} = \left(\frac{\left[4f''\left(1 - A^2\right) + 4A^2 K_m + \frac{2t_{b1}}{\sqrt{6}}\right]\cos\left(k_0\frac{\pi}{2}\right)}{\sqrt{m_U m_{Br}}}\right) ,$$

$$F_{15,15} = \left(\frac{8f'' + 4K_m + 4K_q}{m_{Cs}}\right) ,$$

$$F_{15,17} = -\left(\frac{4A^2(f'' + K_m) - \frac{8t_{b1}}{\sqrt{6}}}{\sqrt{m_{Br} m_{Cs}}}\right) ,$$

$$F_{15,18} = \left(\frac{\left[4A^2(f'' - K_m) - \frac{8t_{b1}}{\sqrt{6}}\right]\cos\left(k_0\frac{\pi}{2}\right)}{\sqrt{m_{Br} m_{Cs}}}\right) ,$$

$$F_{16,16} = \left(\frac{8H + 2K - 2f_r' - 16F_{r\alpha} - 16t_2 + \frac{32t_{b1}}{\sqrt{6}} - 16F'}{m_U}\right) ,$$

$$F_{16,19} = -\left(\frac{\frac{8t_{b1}}{\sqrt{3}}\cos\left(k_0\frac{\pi}{2}\right)}{\sqrt{m_U m_{Cs}}}\right) ,$$

$$F_{17,17} = \left(\frac{4f''\left(1-A^2\right) + 4A^2K_m + 2H + F - F' + f' - 4t_1}{m_{Br}}\right) ,$$

$$F_{17,18} = \left(\frac{2H + F - F' - 4t_1}{m_{Br}}\right) ,$$

$$F_{18,18} = \left(\frac{4f''\left(1-A^2\right) + 4A^2K_m + 2H + F - F' + f' - 4t_1}{m_{Br}}\right) ,$$

$$F_{19,19} = \left(\frac{8f'' + 4K_m}{m_{Cs}}\right) .$$

The compatibility relations are as follows:

A_{1g}	A_{2g}	E_g	T_{1g}	T_{2g}	A_{1u}	A_{2u}	E_u	T_{1u}	T_{2u}
Δ_1	Δ_2	$\Delta_1\Delta_2$	$\Delta_1'\Delta_5$	$\Delta_2'\Delta_5$	Δ_1'	Δ_2'	$\Delta_1'\Delta_2'$	$\Delta_1\Delta_5$	$\Delta_2\Delta_5$
Λ_1	Λ_1	Λ_3	$\Lambda_2\Lambda_3$	$\Lambda_1\Lambda_3$	Λ_2	Λ_1	Λ_3	$\Lambda_1\Lambda_3$	$\Lambda_2\Lambda_3$
Σ_1	Σ_4	$\Sigma_1\Sigma_4$	$\Sigma_2\Sigma_3\Sigma_4$	$\Sigma_1\Sigma_2\Sigma_3$	Σ_2	Σ_3	$\Sigma_2\Sigma_3$	$\Sigma_1\Sigma_3\Sigma_4$	$\Sigma_1\Sigma_2\Sigma_4$

X_1^+	X_2'	X_3'	X_4^+	X_5^+	X_1^-	X_2^-	X_3^-	X_4^-	X_5^-
Δ_1	Δ_2	Δ_2'	Δ_1'	Δ_5	Δ'_1	Δ_2'	Δ_2	Δ_1	Δ_5
Z_1	Z_1	Z_4	Z_4	Z_3Z_4	Z_2	Z_2	Z_3	Z_3	Z_1Z_4
S_1	S_4	S_1	S_4	S_2S_3	S_2	S_3	S_2	S_3	S_1S_4

L_1^+	L_2'	L_3'	L_1^-	L_2^-	L_3^-
Λ_1	Λ_2	Λ_3	Λ_2	Λ_1	Λ_3
Q_1	Q_2	Q_1Q_2	Q_1	Q_2	Q_1Q_2

W_1	W_2	W_1'	W_2'	W_3
Z_1	Z_2	Z_2	Z_1	Z_3Z_4
Q_1	Q_2	Q_1	Q_2	Q_1Q_2

References

1. Torres DI, Freire JD, Katiyar RS (1997) Phys Rev B 56: 7763
2. Born M, Huang K (1945) Dynamical theory of crystal lattices. Oxford University Press, Oxford
3. Johnston DR, Satten RA, Schreiber CL, Wong EY (1966) J Chem Phys 44: 3141
4. Flint CD, Tanner PA (1987) Mol Phys 61: 389
5. Johnston D, Satten RA, Wong E (1966) J Chem Phys 44: 687
6. Satten RA, Schreiber CL, Wong EY (1983) J Chem Phys 78: 79
7. Satten RA, Johnston DR, Wong EY (1968) Phys Rev Sect B 171: 370
8. Chodos SL (1971) PhD thesis. University of California at Los Angeles
9. Chodos SL (1972) J Chem Phys 57: 2712
10. Chodos SL, Satten RA (1975) J Chem Phys 62: 2411
11. Cortés E (1992) DSc thesis. Universidad de Chile
12. Acevedo R, Flint CD, Meruane T, Muñoz G, Pasman M, Poblete V (1997) J Mol Structure (THEOCHEM) 390: 109
13. Chodos SL, Berg R (1979) J Chem Phys 70: 4864
14. Clark C (1958) Phys Rev 109: 1133
15. Cochran W, Cowley R (1967) Handb Phys B 25: 59
16. Chodos SL, Black AM, Flint CD (1976) J Chem Phys 65: 4815
17. O'Leary GP, Wheeler RG (1970) Phys Rev B 1: 4409
18. Kuhner D, Lauer H, Bron W (1972) Phys Rev B 5: 4112
19. Labonville P, Ferraro JR, Wall MC, Basile LJ (1972) Coord Chem Rev 7: 257
20. Acevedo R, Vásquez SO, Pasman M (1994) An Quim 90: 237
21. Acevedo R, Meruane T, Cortés E, Poblete V (1995) An Quim 91: 479
22. Nissen-Sobocinska B, Strek W, Hamiza J, Hermanowicz K, Denisenko G, Aleksandrov KS, Voronow VN (1995) J Appl Spectrosc 62: 94
23. Nissen B, Luxbacher T, Strek W, Flint CD (1999) Chem Phys Lett 303: 235
24. Denning RG, Berry AJ, McCaw CS (1998) Phys Rev B 57: R2021
25. Cracknell AD (1975) Group Theory in solid state physics. Taylor and Francis, London
26. Decius J, Hexter R (1977) Molecular vibrations in crystals. McGraw-Hill, New York
27. Hammersh M (1962) Group theory and its applications to physical problems. Addison-Wesley, Reading, Mass
28. Califano S (1976) Vibrational states. Wiley, London
29. Bhagavantan S, Benkataruyudu T (1969) Theory of groups and its applications to physical problems. Academic, New York
30. Ross SD (1972) Inorganic infrared and Raman spectra. McGraw-Hill, New York
31. Cochran W (1960) Adv Phys 9: 387
32. Satten RA, Young D, Gruen DM (1960) J Chem Phys 33: 1140
33. Pollak SA, Satten RA (1962) J Chem Phys 36: 804
34. Pollak SA (1971) PhD thesis. University of California at Los Angeles
35. Halford R (1946) J Chem Phys 14: 8
36. (a) Flint CD, Tanner PA (1984) Mol Phys 53: 429; (b) Flint CD, Tanner PA (1984) Mol Phys 53: 437; (c) Flint CD, Tanner PA (1984) Mol Phys 53: 801
37. Maradudin AA, et al (1963) Solid state physics. Academic, New York
38. Staffsudd OM (1967) PhD thesis. University of California at Los Angeles
39. Ewald PP (1921) Ann Phys (Leipzig) 64: 253